Original Article

CircMMP9 accelerates the progression of hepatocellular carcinoma through the *miR-149/CCND2* axis

Xiaolou Li[1], Jiankai Fang[1], Guangmin Wei[1], Ying Chen[2], Dongliang Li[3]

[1]Department of Oncology, Mengchao Hepatobiliary Hospital of Fujian Medical University, Fuzhou, China; [2]Outpatient Department, Mengchao Hepatobiliary Hospital of Fujian Medical University, Fuzhou, China; [3]Department of Hepatobiliary Medicine, the 900th Hospital of Joint Logistics Support Forces of the Chinese PLA, Fuzhou, China

Contributions: (I) Conception and design: X Li; (II) Administrative support: D Li; (III) Provision of study materials or patients: X Li, D Li; (IV) Collection and assembly of data: J Fang; (V) Data analysis and interpretation: X Li, G Wei; (VI) Manuscript writing: All authors; (VII) Final approval of manuscript: All authors.

Correspondence to: Dongliang Li. Department of Hepatobiliary Medicine, the 900th Hospital of Joint Logistics Support Forces of the Chinese PLA, 156 West Second Ring North Road, Fuzhou 350025, China. Email: Dongliangli93@163.com.

Background: This study aimed to verify the hypothesis that *circular RNA MMP9* (*circMMP9*) promotes hepatocellular carcinoma (HCC) progression through targeting *miR-149* and regulating cyclin D2 (*CCND2*) expression.

Methods: Expression of *circMMP9*, *miR-149* and *CCND2* was detected by quantitative reverse transcription polymerase chain reaction (qRT-PCR) or protein blotting. Cell Counting Kit-8 (CCK-8) was used to evaluate cell proliferation. The HCC cell migration and invasion were evaluated using wound healing and transwell assays. The interaction among *circMMP9*, *miR-149*, and *CCND2* was evaluated using luciferase, RNA-pull down, and RNA immunoprecipitation (RIP) assays, respectively. Cell apoptosis and cycle were examined by flow cytometry. A subcutaneous HCC xenograft mouse model was established for analyzing the role of *circMMP9* in regulating the progression of HCC *in vivo*.

Results: The expression of *circMMP9* was elevated in HCC tissues and its high expression correlated with poor prognosis (P<0.05). Knockdown of *circMMP9* restrained the proliferation, migration, and invasion of HCC cells and led to arrested cell cycle and increased apoptosis (all P<0.05). Furthermore, knockdown of *circMMP9* attenuated HCC growth *in vivo* (P<0.05). Mechanically, *circMMP9* acted as a sponge for *miR-149* and enhanced *CCND2* expression in HCC cells (P<0.05). Inhibition of *miR-149* or overexpression of *CCND2* abrogated knockdown of *circMMP9*-mediated alleviation of the malignant phenotypes of HCC (P<0.05).

Conclusions: For the first time, we demonstrated that *circMMP9* exacerbated HCC progression through the *miR-149/CCND2* axis, which suggested that *circMMP9* could be potentially targeted for HCC treatment.

Keywords: *Circular RNA MMP9* (*circMMP9*); hepatocellular carcinoma (HCC); invasion; *miR-149*; cyclin D2 (CCND2)

Submitted Nov 18, 2021. Accepted for publication Aug 05, 2022.
doi: 10.21037/jgo-22-677
View this article at: https://dx.doi.org/10.21037/jgo-22-677

Introduction

Hepatocellular carcinoma (HCC) is one of the most aggressive carcinomas and causes a great number of deaths each year worldwide (1,2). High malignancy of HCC is the primary cause of therapeutic failure and leads to poor prognosis (3,4). Although advances have been made in HCC therapies including surgery, targeted drug therapy, and immunotherapy, the therapeutic effect is still unsatisfactory, especially for patients with advanced HCC. Therefore, elucidating the underlying mechanisms of HCC progression is vital for developing novel therapies for HCC.

Circular RNAs (circRNAs) are non-coding RNAs

with covalently linked 5' and 3' termini and have been demonstrated to exert vital functions in various biological processes (5,6). Intriguingly, one study has demonstrated that circRNAs exert key functions in regulating the progression of various human cancers (7). Pan *et al.* reported that the expression of *circRNA MMP9* (*circMMP9*) was elevated in osteosarcoma, and knockdown of *circMMP9* restrained the proliferation, migration, and invasion of osteosarcoma cells (8). Moreover, *circMMP9* strengthens the migratory and invasive capacities of glioblastoma multiforme cells (9). The circRNAs can be developed as diagnostic and prognostic markers and therapeutic targets for HCC (10-12); however, the function of *circMMP9* and related molecular mechanisms in HCC are unknown.

MicroRNAs (miRNAs) are small non-coding RNAs of approximately 22 nt in length and work as key regulators in gene expression (13). It has been well accepted that circRNAs regulate cancer progression via acting as miRNA sponges and reducing the expression of downstream targets (14,15). The *circMMP9* promotes the progression of osteosarcoma and glioblastoma multiforme by sponging *miR-1265* and *miR-124*, respectively (8,9). Importantly, miRNAs serve as important regulators in various human carcinomas (16,17). It has been reported that *miR-149* is dysregulated in various carcinomas (18). The expression of *miR-149* is downregulated in breast cancer tissues, and its suppression accelerates the progression of breast cancer (19). Xu *et al.* demonstrated that *miR-149* weakens the migration and invasion of colorectal cancer cells via targeting *FOXM1* (20). Additionally, *miR-149* attenuates the metastasis of HCC via sponging *PPM1F* (21). Considering the important roles of *miR-149* in various cancers including HCC, more studies are required to elucidate the function of *miR-149* in HCC and evaluate the potential interaction between *circMMP9* and *miR-149* in HCC.

As a member of the cyclin family, cyclin D2 (*CCND2*) is a key regulator in cell cycle progression and proliferation (22), and it has been implicated in liver regeneration (23). In addition, the expression of *CCND2* is inhibited in early recurrent HCC, and methylated *CCND2* in the serum could be a prognostic indicator of HCC (24). Besides, our preliminary data suggested that *miR-149* might bind to *circMMP9* and *CCND2*. Therefore, the *circMMP9/miR-149/CCND2* axis may be implicated in the progression of HCC. Herein, we hypothesized that *circMMP9* may promote HCC progression through targeting *miR-149* and subsequently regulating *CCND2* expression. The knowledge of the pathogenesis of hepatocellular carcinoma (HCC) is limited. Surgery or transplantation are effective treatments, but recurrence and metastasis rates remain high, and 5-year survival rates are low (25). Many circRNAs are involved in the processes of HCC cell proliferation, invasion, and migration. As a result, circRNA may be a useful biomarker in the clinical diagnosis and treatment of HCC. To our knowledge, this is the first report of the role *circMMP9* in HCC and it provides potential therapeutic targets for HCC. We present the following article in accordance with the ARRIVE reporting checklist (available at https://jgo.amegroups.com/article/view/10.21037/jgo-22-677/rc).

Methods

Patients

Tumor and adjacent normal (NC) tissues were obtained from 70 HCC patients at Mengchao Hepatobiliary Hospital of Fujian Medical University. The tissues were frozen and stored at –80 ℃ for analysis of the expression of *circMMP9*. The overall survival (OS) of these patients was monitored. Participant clinical pathological characteristics are shown in *Table 1*. The study was conducted in accordance with the Declaration of Helsinki (as revised in 2013). The study was approved by the Institutional Ethics Review Board of Mengchao Hepatobiliary Hospital of Fujian Medical University (No. 2020-035-01) and informed consent was taken from all the patients.

Cell culture and transfection

The Cell Bank of the Chinese Academy of Sciences (Shanghai, China) provided normal human hepatic cells L02 and HCC cells Huh7, HepG2, HCCLM3, and Hep3B. All of these cells were grown in Dulbecco's modified Eagle's medium (DMEM; HyClone, Logan, UT, USA) with 12% fetal bovine serum (FBS; HyClone). To establish stable *circMMP9*-silencing cells, short hairpin RNAs (shRNAs) against *circMMP9* (sh-*circMMP9*#1, #2, and #3) were cloned into the pLKO.1 lentiviral vector and lentiviral particles were generated. As a negative control, an empty lentiviral vector (sh-NC) was used. Then, Huh7 and Hep3B cells were infected with lentiviral particles for stable expression of sh-*circMMP9*. The coding region of *CCND2* was inserted into the pcDNA3.1 vector. The Huh7 and Hep3B cells were transfected with the *CCND2* overexpressing vector using Lipofectamine 3000 reagents (Thermo Fisher Scientific, Waltham, MA, USA). Cells were transfected with

Table 1 Correlation between *circMMP9* expression and the clinical pathological features of 70 HCC patients

Characteristics	All cases (n=70)	*CircMMP9* expression		P value
		High (n=35)	Low (n=35)	
Gender				0.212
Male	45	20	25	
Female	25	15	10	
Age (years)				0.467
<60	29	13	16	
≥60	41	22	19	
Tumor size (cm)				0.460
<5	27	15	12	
≥5	43	20	23	
Differentiation				0.016*
Well/moderate	30	10	20	
Poor	40	25	15	
HBsAg				0.803
Positive	45	22	23	
Negative	25	13	12	
TNM stages				0.030*
I/II	39	15	24	
III/IV	31	20	11	

Data were analyzed by chi-squared test. *P<0.05. *CircMMP9*, *circular RNA MMP9*; HCC, hepatocellular carcinoma; HBsAg, hepatitis B surface antigen; TNM, tumor-node-metastasis.

Table 2 The sequence of reagents used in cell transfection

Name	Sequence (5'-3')
MiR-149 mimics	UCUGGCUCCGUGUCUUCACUCCC
Mimics NC	UCGCUUGGUGCAGGUCGGGAA
MiR-149 inhibitor	GGGAGTGAAGACACGGAGCCAGA
Inhibitor NC	CAGUACUUUUGUGUAGUACAA
sh-*circMMP9*#1	GTGGAGGCGCAGATGGTGGAT
sh-*circMMP9*#2	AGGAGTGGAGGCGCAGATGGT
sh-*circMMP9*#3	GGGAGGAGTGGAGGCGCAGAT
sh-NC	UAAGGCUAUGAAGAGAUAC

CircMMP9, *circular RNA MMP9*; NC, adjacent normal; sh, short hairpin.

Table 3 qRT-PCR primers in this study

Name	Sequence (5'-3')
CircMMP9	5'-CCAGTTACAAGTTTAGGGCTGT-3'
	5'-TGTCTCCATTTGCTTCTTCTTCA-3'
MiR-149	5'-CATCCTTTCTGGCTCCGTGT-3'
	5'-GCGTGATTCGTGCTCGTATATC-3'
U6 snRNA	5'-CTCGCTTCGGCAGCACA-3'
	5'-AACGCTTCACGAATTTGCGT-3'
GAPDH	5'-TGCACCACCAACTGCTTAGC-3'
	5'-GGCATGGACTGTGGTCATGAG-3'

qRT-PCR, quantitative reverse-transcription polymerase chain reaction; *CircMMP9*, *circular RNA MMP9*.

miR-149 mimics, inhibitor or negative controls (mimics and inhibitor NC) from RiboBio (Guangzhou, China) using Lipofectamine RNAiMAX (Thermo Fisher). The sequence of reagents used in cell transfection is listed in *Table 2*.

Real-time quantitative reverse-transcription polymerase chain reaction (qRT-PCR)

The RNA was isolated from tumor and NC tissues from HCC patients and cells using TRIzol™ LS Reagent (Thermo Fisher) followed by RNA quantification. The RNA was subsequently reversely transcribed into complementary DNA (cDNA). Then, miRNA was isolated using mirPremier miRNA Isolation Kit (Merck, St. Louis, MO, USA) and reversely transcribed into cDNA with the miScript kit from QIAGEN (Germantown, MD, USA). We then quantified *circMMP9* and *miR-149* by real-time PCR and normalized to glyceraldehyde 3-phosphate dehydrogenase (*GAPDH*) or U6 snRNA. The PCR reaction system (20 μL) was as follows: 2 μL of cDNA template, 7.5 μL of ddH_2O, 0.5 μL of paired primers (final concentration: 0.3 μM), and 10 μL of SYBR green. The PCR condition was as follows: initial denaturation at 94 ℃ for 3 min; 35 cycles of denaturation at 94 ℃ for 15 s, annealing at 60 ℃ for 30 s and elongation at 72 ℃ for 15 s; and final elongation at 72 ℃ for 3 min. The $2^{-\Delta\Delta Ct}$ method was used for analyzing gene expression. Primers are shown in *Table 3*.

RNase R digestion

Total RNA was isolated from Hep3B and HuH7 cells. We used RNase R (4 U/μg, Sigma-Aldrich, St. Louis, MO,

USA) for digesting total RNA (5 μg) at 37 ℃ for 20 min. The RNA was then purified. Both *circMMP9* and *GAPDH* were examined by qRT-PCR.

A subcutaneous HCC xenograft mouse model

The BALB/c nude mice (10-week-old, male) were provided by the Animal Center of Fujian Medical University. The subcutaneous HCC xenograft mouse model was established as previously described (26). The Huh7 cells were lentivirally transfected with sh-NC or sh-*circMMP9*, and 2×10^6 cells were subcutaneously injected into the mice's left flanks. On days 7, 14, 21, 28, and 35, the tumor size was measured. Tumor volume was calculated using the formula length width width^2/2. Mice were euthanized by adjusting CO_2 flow into cages at 3 L/min until death, and tumors were excised and weighed. All animal procedures were approved by the Animal Care and Use Committee of Fujian Medical University (No. 2019009), in compliance with the institutional guidelines for the care and use of animals.

Luciferase activity

Wild-type (WT) or mutant (MUT) binding sites for *miR-149* in *circMMP9* and the *CCND2* 3' untranslated region (3' UTR) was inserted into the pmirGLO vector (Promega, Madison, WI, USA). Huh7 and Hep3B cells were co-transfected with the luciferase reporter *circMMP9* or *CCND2* as well as miR-149 mimics. We used NC mimics as a control. At 48 h post-transfection, cells were collected, and the Dual-Glo system (Promega) was used to examine the luciferase activity.

Cell Counting Kit-8 (CCK-8) assay

Transfection of Huh7 and Hep3B cells with sh-*circMMP9*, sh-*circMMP9* + *miR-149* inhibitor (anti-*miR-149*) or sh-*circMMP9* + *CCND2* overexpressing vector (*CCND2*) and seeded in 96-well plates. We used sh-NC as a control. At 24, 48, and 72 h, culture media were replaced. The CCK-8 from Dojindo (Rockville, MD, USA) was added and incubated for 4 h before measuring absorbance reading at 450 nm.

Cell cycle and apoptosis

Cell cycle was examined using FxCycle™ propidium iodide (PI)/RNase Staining Solution (Thermo Fisher) according to the manual. Cells were fixed in 75% ethanol solution and PI/RNAse solution was added into cells. Subsequently, cells were incubated for 30 min protected from light. The cell apoptosis kit was bought from Solarbio (Beijing, China). Cells were suspended and stained with FITC-Annexin V and PI for 20 min. Cell cycle and apoptosis were examined using a flow cytometer [Becton, Dickinson, and Co. (BD), Franklin Lakes, NJ, USA].

Transwell assay

Cell invasion was evaluated through the transwell assay. We seeded 1×10^5 Huh7 and Hep3B cells into the upper chamber precoated with Matrigel (BD) and incubated them for 24 h. Subsequently, invasive cells in the lower chamber were stained with crystal violet (Sigma) and imaged with a BX51 microscope (Olympus, Tokyo, Japan). Transwell chambers (8 μm-pore) were obtained from Corning (Corning, NY, USA).

Wound healing assay

Cell migration was evaluated by the wound healing assay. The Huh7 and Hep3B cells were seeded and grown to form a confluent monolayer. After removing the culture medium, the cell monolayer was scraped with cell combs (EMD Millipore, Darmstadt, Germany). Cells were then cultured for additional 24 h and observed with a BX51 microscope (Olympus), which was quantified using the Image J software (https://imagej.nih.gov/ij/download.html).

RNA immunoprecipitation (RIP) assay

The Huh7 and Hep3B cells were lysed, and supernatants were harvested after centrifugation. An Ago-2 antibody or normal IgG isotype was coated on magnetic beads and added into supernatants. Samples were incubated with gentle rotation overnight. The RNA was recovered using TRIzol™ LS Reagent (Thermo Fisher), and the enrichment of *circMMP9* and *miR-149* were examined by qRT-PCR.

RNA pull-down

Thermo Fisher provided a magnetic RNA-protein pull-down kit, which was used to investigate the interaction between *circMMP9* and *miR-149*. The Huh7 and Hep3B cells were lysed. Subsequently, supernatants were harvested, and biotin-labeled *miR-149* probes were added. After

incubation for 5 h at 4 ℃, magnetic beads conjugated with streptavidin were added and incubated for an additional 2h.

Western blot

The Huh7 and Hep3B cells were transfected with *miR-149* mimics, mimics NC, *miR-149* inhibitor, inhibitor NC, sh-NC, sh-*circMMP9*, and sh-*circMMP9* + anti-*miR-149* or sh-*circMMP9* + *CCND2*, respectively. Cells were then lysed, and cell lysates were obtained. Protein was quantified using the BCA kit from Santa Cruz (Dallas, TX, USA). Protein was electrophoresed and transferred to PVDF membranes (Bio-Rad, Hercules, CA, USA). Membranes were blocked and incubated with a *CCND2* antibody (1:1,000, Abcam, Cambridge, UK). Following that, the membranes were washed and incubated with a secondary antibody conjugated to horseradish peroxidase (HRP) (Santa Cruz). To observe the bands, the ECL substrate (Bio-Rad) was used.

Statistical analysis

In this study, results were gathered from three independent assays and presented as mean standard deviation. The Student's *t*-test and one-way analysis of variance (ANOVA) were used to determine the significance of variance in two and multiple groups, respectively. The Bonferroni post hoc test was used to compare two groups in multiple groups. The Kaplan-Meier plotter was used to compare the survival of patients with high and low *circMMP9* expression. *P<0.05, **P<0.01 and ***P<0.001. A P value <0.05 was considered statistically significant.

Results

Elevated expression of circMMP9 was associated with the poor prognosis of patients with HCC

We collected tumor and NC tissues from HCC patients and analyzed the expression of circMMP9 to investigate the function of circMMP9 in HCC. CircMMP9 expression was significantly increased in tumor tissues (*Figure 1A*). Participants were divided into two groups based on the median expression of *circMMP9* in tumor tissues: *circMMP9*^{high} and *circMMP9*^{low}. The survival of *circMMP9*^{high} patients was obviously less favorable than that of *circMMP9*^{low} patients (*Figure 1B*), suggesting that increased expression of *circMMP9* was associated with the poor prognosis of HCC patients. The expression of *circMMP9* was markedly correlated with tumor differentiation and tumor-nodes-metastases (TNM) stage rather than gender, age, tumor size, and hepatitis B surface antigen (HBsAg) (*Table 1*). We also found the expression of *circMMP9* was significantly increased in HCC cells including Huh7, HepG2, HCCLM3, and Hep3B compared to that in L02 cells (*Figure 1C*). As Huh7 and Hep3B cells showed highest expression of *circMMP9*, they were selected for subsequent assays. As circRNAs are resistant to RNase R digestion, total RNA from Huh7 and Hep3B cells were treated with RNase R or mock (27). The qRT-PCR analysis showed that *circMMP9*, but not *GAPDH*, was resistant to RNase R digestion (*Figure 1D*), indicating that *circMMP9* was a circRNA.

Knockdown of circMMP9 reduced HCC cell proliferation, induced cell cycle arrest and apoptosis in vitro and attenuated tumor growth in vivo

The *circMMP9* was knocked down in Huh7 and Hep3B cells by lentiviral transduce of sh-*circMMP9*#1, #2, and #3. The expression of *circMMP9* was efficiently suppressed in Huh7 and Hep3B cells, and the lowest expression of *circMMP9* was observed in cells transfected with sh-circMMP#1 (*Figure 2A*). Therefore, sh-*circMMP9*#1 was used for subsequent knockdown of *circMMP9*. Knockdown of *circMMP9* reduced Huh7 and Hep3B cell proliferation (*Figure 2B*). The Huh7 and Hep3B cells at G0/G1 stage were increased and cells at S stage were reduced by knockdown of *circMMP9* (*Figure 2C*), suggesting that knockdown of *circMMP9* caused cell cycle arresting at G0/G1 stage. Besides, apoptotic cell rate was obviously elevated in HCC cells by knockdown of *circMMP9* (*Figure 2D*). Then, Huh7 cells transfected with sh-NC or sh-*circMMP9* were subcutaneously injected into mice for evaluating tumor growth *in vivo*. Tumor volume and weight formed by Huh7 cells were dramatically suppressed by knockdown of *circMMP9* (*Figure 2E,2F*). These data demonstrated that knockdown of *circMMP9* attenuated tumor growth *in vivo*.

Knockdown of circMMP9 inhibited HCC cell migration and invasion

Wound healing and transwell assays were performed to study whether knockdown of *circMMP9* affects HCC cell migration and invasion. Cell migration was notably reduced in cells with knockdown of *circMMP9* compared to that

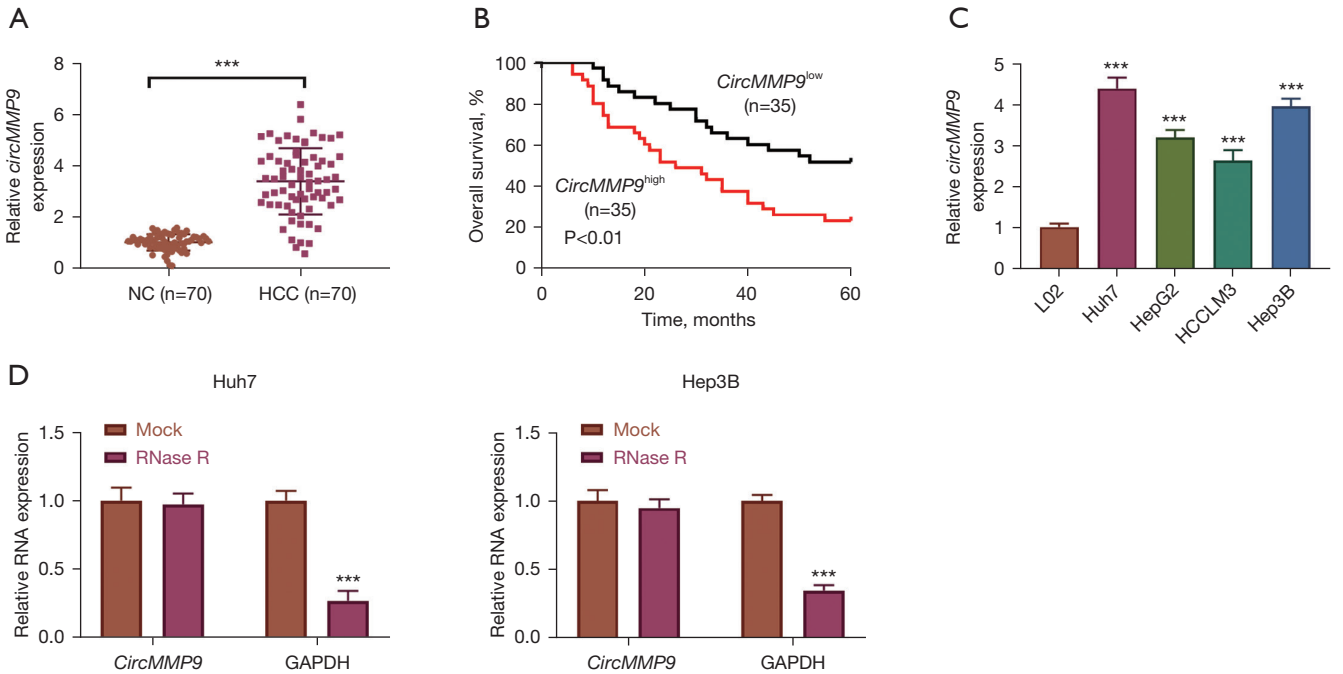

Figure 1 *CircMMP9* was highly expressed in HCC tissues and cells. (A) The expression of *circMMP9* in HCC and NC tissues were analyzed by qRT-PCR (n=70); (B) the Kaplan-Meier plotter was applied to analyze the survival variance between patients (*circMMP9*^{high} and *circMMP9*^{low}); (C) the expression of *circMMP9* in L02, Huh7, HepG2, HCCLM3 and Hep3B cells were assessed by qRT-PCR; (D) qRT-PCR analysis of *circMMP9* and *GAPDH* after RNase R or mock treatment (n=3). ***P<0.001, compared to *circMMP9* expression in L02 cells, n=3. *CircMMP9*, *circular RNA MMP9*; HCC, hepatocellular carcinoma; NC, adjacent normal; qRT-PCR, quantitative reverse-transcription polymerase chain reaction.

of cells transfected with sh-NC (*Figure 3A*). Furthermore, cells with knockdown of *circMMP9* exhibited lower invasive capacity than control cells (*Figure 3B*). Collectively, knockdown of *circMMP9* suppressed HCC cell migration and invasion.

CircMMP9 sponged miR-149 in HCC cells

Nuclear and cytoplasmic fractions of Huh7 and Hep3B cells were separated, and the enrichment of *circMMP9*, U6, and *GAPDH* were evaluated using qRT-PCR. Same as *GAPDH*, *circMMP9* mainly localized in the cytoplasm (*Figure 4A*). As circRNAs act as sponges for miRNAs, we predicted that *miR-149* might be a novel target of *circMMP9* using CircInteractome (*Figure 4B*) (28). The WT circMMP9 reporter's luciferase activity, but not the MUT circMMP9 reporter, was inhibited by overexpression of *miR-149* (*Figure 4C*). In addition, compared to the control probe, the *miR-149* probe efficiently enriched *circMMP9* from Huh7 and Hep3B cell lysates (*Figure 4D*). The RIP assays showed that both *circMMP9* and *miR-149* were enriched in the anti-Ago2-immunoprecipitated complex (*Figure 4E*). It was concluded that *circMMP9* could sponge *miR-149* in HCC cells.

MiR-149 targeted CCND2 to reduce its expression in HCC cells

StarBase v2.0 (https://bio.tools/starbase) was used to find downstream targets of *miR-149* in HCC, and we discovered a potential *miR-149* binding site in the 3' UTR of *CCND2* (*Figure 5A*). The luciferase assay revealed that overexpression of miR-149 inhibited the luciferase activity of the WT *CCND2* reporter, but not after the binding site was mutated (*Figure 5B*). The expression of *CCND2* was reduced in *miR-149* overexpressing cells compared to that in cells transfected with mimics NC (*Figure 5C*). The *miR-149* was knocked down by transfection of *miR-149* inhibitor in Huh7 and Hep3B cells (*Figure 5D*), and the expression of *CCND2* was elevated by knockdown of *miR-149* (*Figure 5E*).

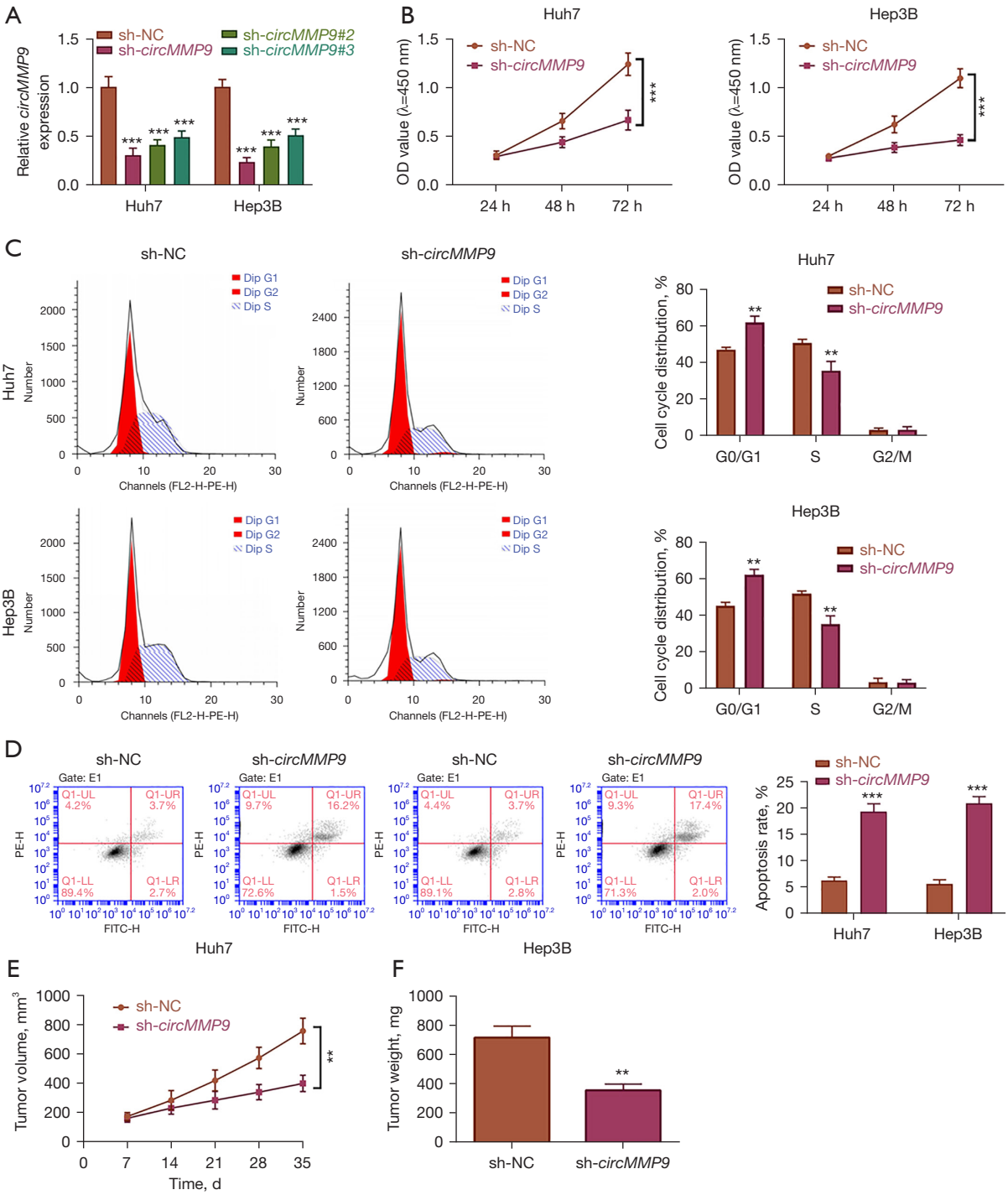

Figure 2 Knockdown of *circMMP9* suppressed HCC cell proliferation, induced cell cycle arrest and apoptosis, and attenuated tumor growth. Huh7 and Hep3B cells were transfected with sh-NC or sh-*circMMP9*. (A) qRT-PCR analysis of *circMMP9* (n=3); (B) cell proliferation was analyzed using CCK-8 at 24, 48 and 72 hours (n=3); (C) cell cycle analysis (n=3); (D) cell apoptosis analysis (n=3); (E) Huh7 cells were transfected with sh-NC or sh-*circMMP9* and subcutaneously injected into mice. The tumor size was measured at day 7, 14, 21, 28 and 35 (n=8); (F) tumor weight (n=8). **P<0.01 and ***P<0.001 for comparing variance between sh-NC and sh-*circMMP9* groups. *CircMMP9*, *circular RNA MMP9*; HCC, hepatocellular carcinoma; sh, short hairpin; NC, adjacent normal; qRT-PCR, quantitative reverse-transcription polymerase chain reaction; G0, cell resting phase; G1, end of last split; S, DNA synthesis period; G2, late DNA synthesis; M, mitotic phase.

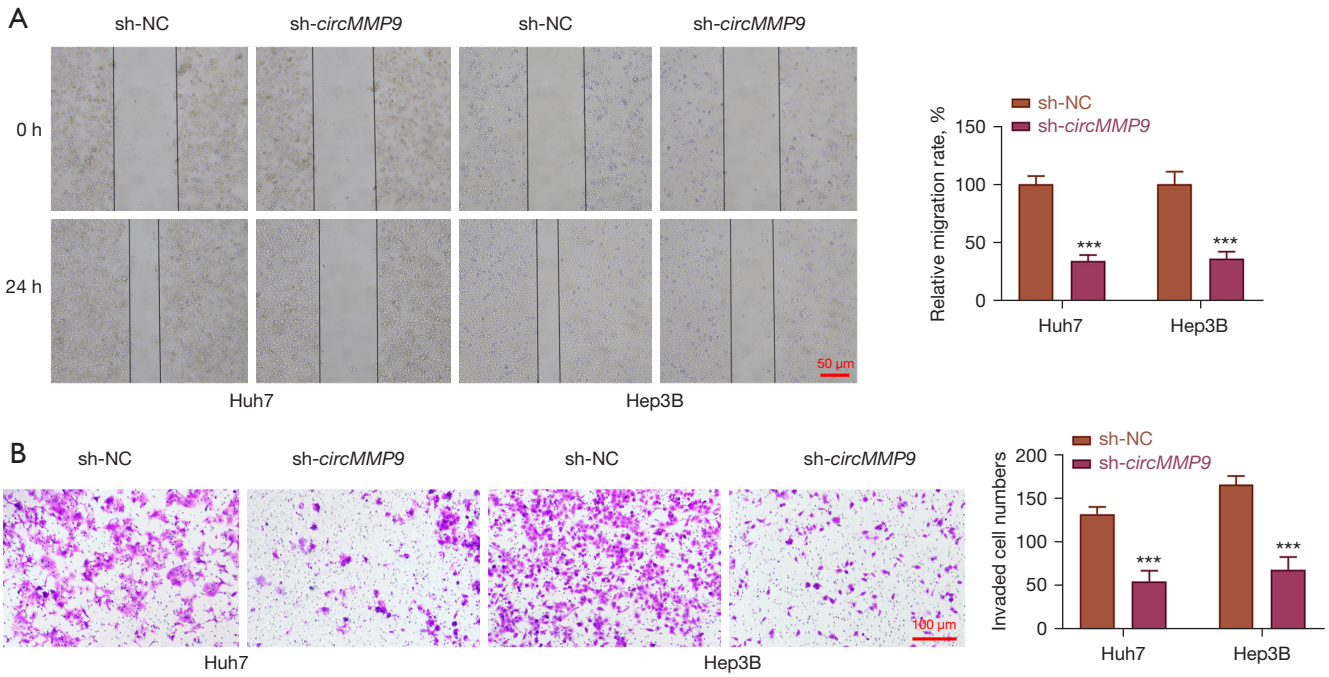

Figure 3 Knockdown of *circMMP9* inhibited HCC cell migration and invasion. (A) Cell migration was analyzed using the wound healing assay (scale bar =50 μm, magnification, 100×, n=3). The monolayers formed by Huh7 and Hep3B cells transfected with sh-NC or sh-*circMMP9* were wounded and cultured for 24 h for healing; (B) cell invasion was analyzed using the transwell assay (scale bar =100 μm, magnification, 200×, n=3). A total of 1×10^5 Huh7 and Hep3B cells transfected with sh-NC or sh-*circMMP9* were seeded into the upper chamber and incubated for 24 hours. Invasive cells in the lower chamber were stained with crystal violet solution. ***P<0.001 for comparing variance between sh-NC and sh-*circMMP9* groups. *CircMMP9*, *circular RNA MMP9*; HCC, hepatocellular carcinoma; sh, short hairpin; NC, adjacent normal.

Taken together, *miR-149* targeted *CCND2* to suppress its expression in HCC cells.

Knockdown of circMMP9 attenuated HCC malignant phenotypes through the miR-149/CCND2 axis

To investigate whether knockdown of *circMMP9*-mediated alleviation of HCC progression was dependent on the *miR-149/CCND2* axis, Huh7 and Hep3B cells were transfected with sh-*circMMP9* and an inhibitor of *miR-149* or the *CCND2* overexpressing vector. The expression of *CCND2* was decreased in Huh7 and Hep3B cells with knockdown of *circMMP9*, but it was reversed by concomitant suppression of *miR-149* or overexpression of *CCND2* (*Figure 6A*). Knockdown of *circMMP9*-mediated inhibition of HCC cell proliferation was abrogated by silencing of *miR-149* or overexpression of *CCND2* (*Figure 6B*). Additionally, knockdown of *circMMP9*-induced cell cycle arrest and apoptosis were reversed by concomitant suppression of *miR-149* or overexpression of *CCND2* in Huh7 and Hep3B cells (*Figure 6C,6D*). Both cell migration and invasion of HCC were mitigated by knockdown of *circMMP9*, which was abolished by concomitant suppression of *miR-149* or overexpression of *CCND2* (*Figure 6E-6G*). These data indicated that knockdown of *circMMP9* attenuated HCC progression through the *miR-149/CCND2* axis.

Discussion

The malignancy of HCC is a highly lethal hepatic carcinoma and the second leading cause of cancer-related death globally, posing a severe health threat and huge economic pressures (29,30). Elucidating the regulatory mechanism of HCC progression is vital for improving the prognosis and developing novel therapies for HCC. CircRNA has distinct structural and biological properties and is no longer thought to be a byproduct of the splicing process. It has important pathological and physiological

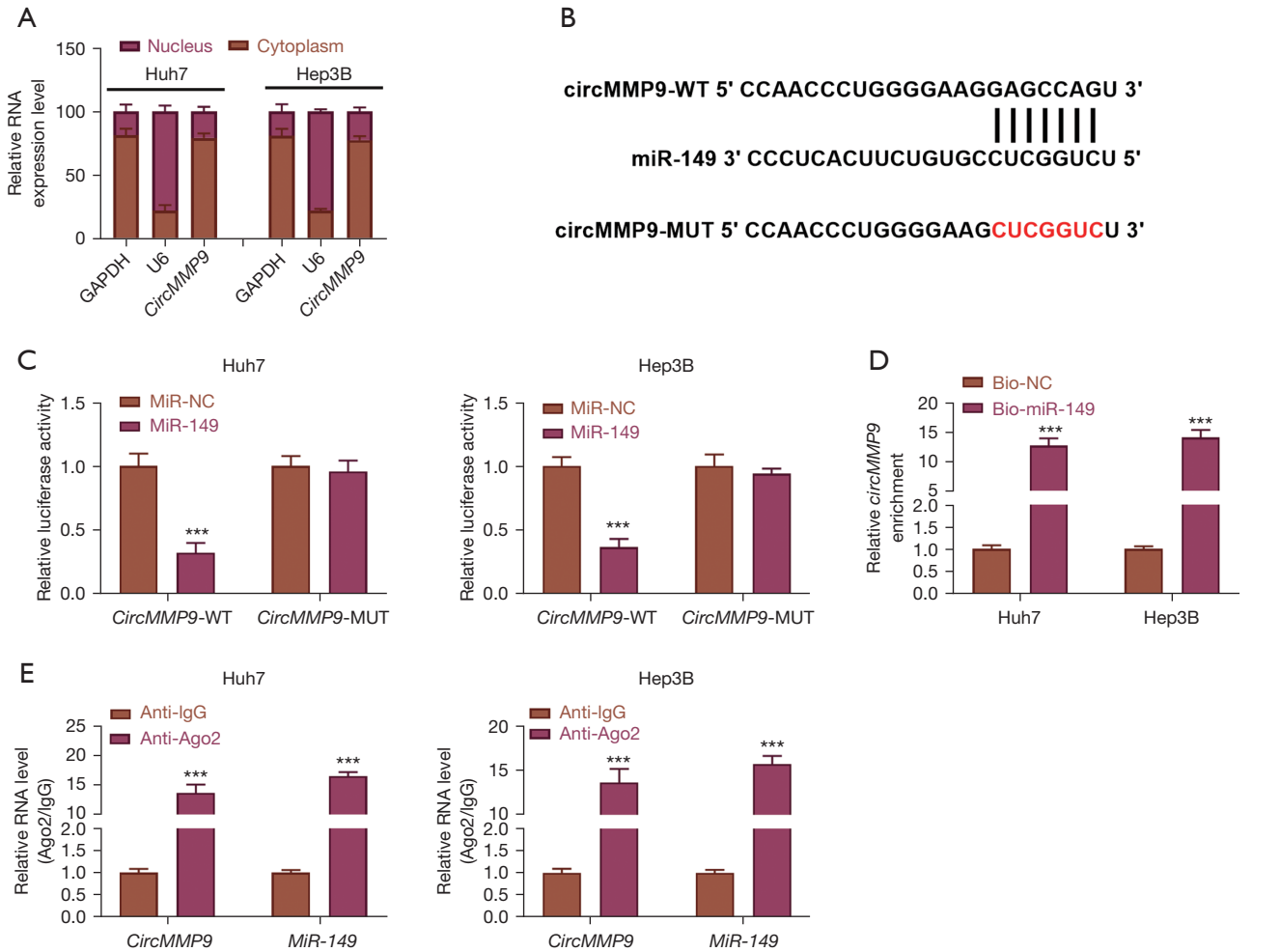

Figure 4 *CircMMP9* targeted *miR-149* in HCC cells. (A) Nuclear and cytoplasmic fractions from Huh7 and Hep3B cells were separated. qRT-PCR analysis of *circMMP9* in cytoplasmic and nuclear fractions (n=3). *GAPDH* and U6 snRNA were used as reference controls; (B) a binding site for *miR-149* in *circMMP9* was predicted by CircInteractome; (C) luciferase activity in Huh7 and Hep3B cells (n=3); (D) enrichment of *circMMP9* by *miR-149* probes (n=3); (E) enrichment of *circMMP9* and *miR-149* in the Ago2 antibody-immunoprecipitated fractions (n=3). ***P<0.001. *CircMMP9*, *circular RNA MMP9*; HCC, hepatocellular carcinoma; qRT-PCR, quantitative reverse-transcription polymerase chain reaction.

roles in various tumors and plays an important regulatory role in them. According to one study, circRNAs act as miRNA adsorption sponges to counteract miRNA-mediated inhibition of mRNA expression (31). The role of the circRNA/miRNA/mRNA regulatory axis in the development and metastasis of HCC is gradually becoming clear (32,33). Previous research has found that a large number of ncRNAs, including circRNAs and miRNAs, are dysregulated in HCC (34-36). In present study, we reported that *circMMP9* sponges *miR-149* and enhances the expression of *CCND2*, thus accelerating the progression of HCC for the first time (*Figure* 7). We provide an experimental and theoretical foundation for HCC targeted therapy using circRNAs/miRNA/mRNA networks.

Increasing evidence has shown that circRNAs are implicated in various human carcinomas including HCC (37-39). The current study of circRNAs faces the following challenges: (I) most current research on circRNA mechanisms has focused on miRNAs acting through the circRNA/miRNA/mRNA regulatory axis, with few reports on other mechanisms. CircRNAs, on the other hand, are translatable, resulting in the production of specific proteins.

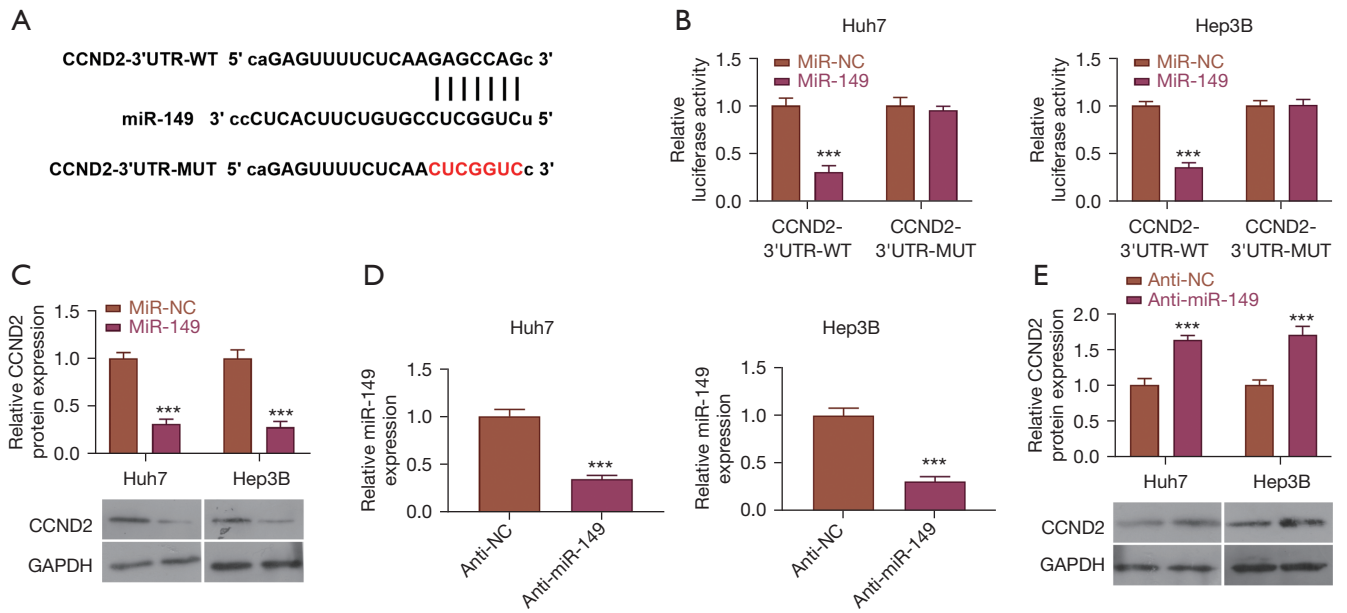

Figure 5 *MiR-149* targeted the 3' UTR of *CCND2* to inhibit its expression in HCC. (A) *CCND2* was predicted to be targeted by *miR-149*; (B) luciferase activity in Huh7 and Hep3B cells (n=3); (C) the expression of *CCND2* in Huh7 and Hep3B cells transfected with mimics NC or *miR-149* mimics were examined by western blot (n=3); (D) qRT-PCR analysis of *miR-149* in Huh7 and Hep3B cells transfected with inhibitor NC (anti-NC) or *miR-149* inhibitor (anti-*miR-149*, n=3); (E) the expression of *CCND2* in Huh7 and Hep3B cells transfected with anti-NC or anti-*miR-149* was examined by western blot (n=3). ***P<0.001. 3' UTR, 3' untranslated region; *CCND2*, cyclin D2; HCC, hepatocellular carcinoma; qRT-PCR, quantitative reverse-transcription polymerase chain reaction; NC, adjacent normal.

As a new field in life sciences, encoding cyclic RNAs may become a potential therapeutic target for liver cancer. (II) At the moment, most studies focus on circRNAs and their regulated downstream target genes, with few reports on the upstream regulators that regulate circRNAs. For instance, Huang *et al.* found that *circRNA_104348* promoted the proliferation, migration, and invasion of HCC cells and inhibited HCC cell apoptosis via targeting *miR-187-3p* and triggering Wnt/β-catenin signaling (40). The *circMTO1* attenuates the progression of HCC through sponging miR-9 and enhancing the expression of p21 (41). Intriguingly, *circMMP9* is upregulated in various cancers such as glioblastoma multiforme and osteosarcoma and acts as an oncogene to promote their progression (8,9). In consistence, we firstly reported that *circMMP9* is highly expressed in HCC and its high expression indicates the poor prognosis of patients with HCC. In addition, Pan *et al.* reported that knockdown of *circMMP9* suppressed osteosarcoma cell proliferation, migration, and invasion and induced its apoptosis (8). Therefore, we examined whether knockdown of *circMMP9* exhibits an anti-tumor activity in HCC. We observed that knockdown of *circMMP9* suppressed malignant phenotypes including proliferation, migration, and invasion of HCC cells. Importantly, knockdown of *circMMP9* restrained HCC growth *in vivo*. Consistent with previous studies, our study supports the notion that *circMMP9* works as an oncogene to enhance cancer progression.

The competitive endogenous RNA (ceRNA) hypothesis has been proposed to describe the crosstalk among non-coding RNAs, which titrates out miRNAs to regulate the expression of downstream targets (42). The circRNAs can function as ceRNAs to target miRNAs and regulate the expression of target genes in cancers (43). The *circMMP9* has been demonstrated to exert its oncogenic activity through acting as sponges for miRNAs including *miR-149*, *miR-1265*, and *miR-124* (8,9,44). Consistently, we observed that *circMMP9* sponged *miR-149* to reduce its expression in HCC cells, identifying *miR-149* as a novel target of *circMMP9* in HCC. Mounting evidence supports that *miR-149* functions as a tumor suppressor in several cancers, including HCC (45-47). We found that silencing of *miR-*

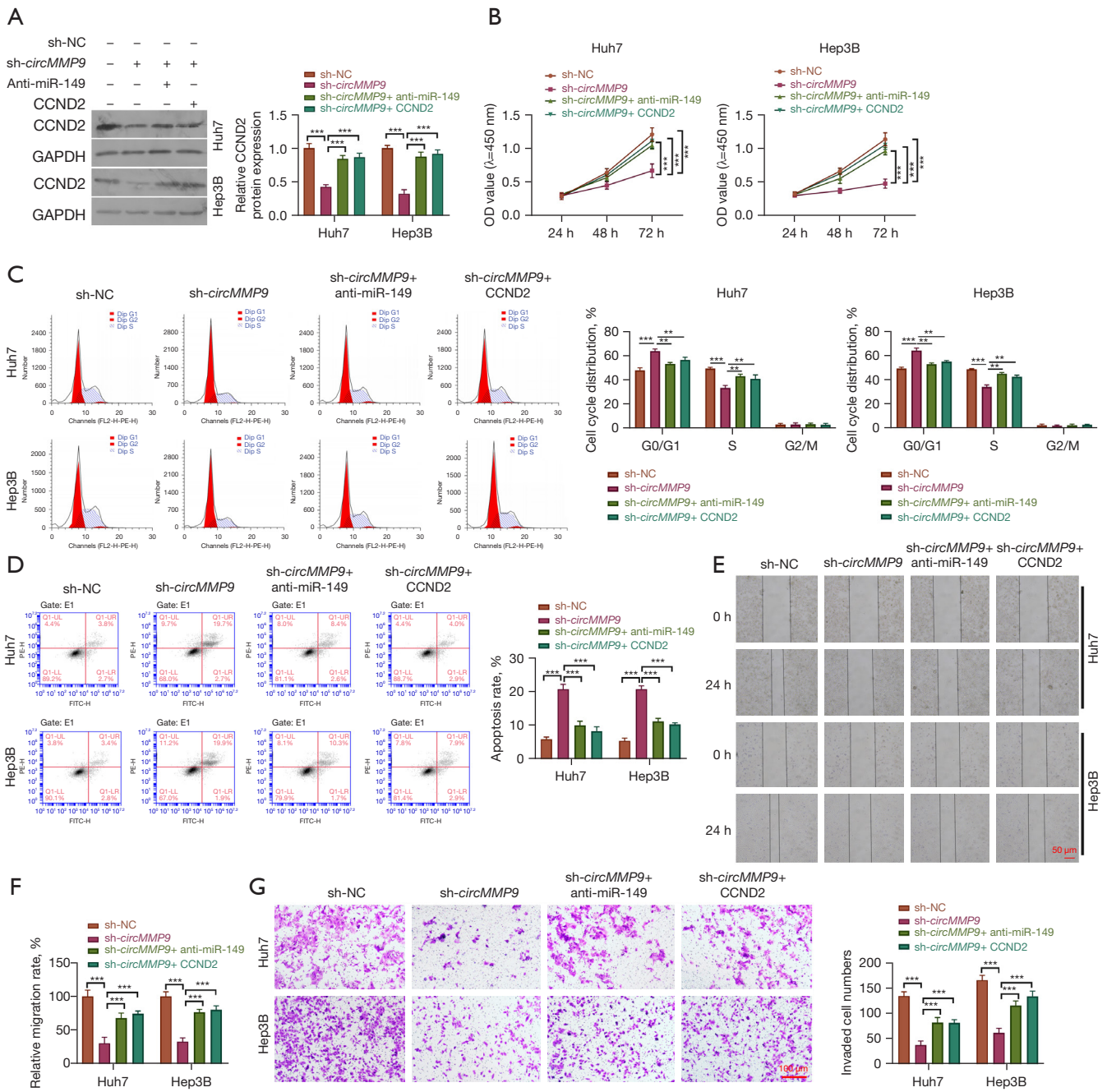

Figure 6 Knockdown of *miR-149* and overexpression of *CCND2* reversed *circMMP9* knockdown-mediated attenuation of HCC malignant phenotypes. Huh7 and Hep3B cells were transfected with sh-NC, sh-*circMMP9*, sh-*circMMP9* + anti-*miR-149* or sh-*circMMP* + *CCND2*, respectively. (A) *CCND2* was examined by western blot; (B) cell proliferation was analyzed using CCK-8 at 24, 48, and 72 h (n=3); (C) cell cycle analysis (n=3); (D) cell apoptosis analysis (n=3); (E,F) cell migration analysis (scale bar =50 μm, magnification, 100×, n=3); (G) cell invasion analysis (crystal violet staining, scale bar =100 μm, magnification, 200×, n=3). **P<0.01 and ***P<0.001. *CCND2*, cyclin D2; *circMMP9*, *circular RNA MMP9*; HCC, hepatocellular carcinoma; sh, short hairpin; NC, adjacent normal; CCK-8, Cell Counting Kit-8; G0, cell resting phase; G1, end of last split; S, DNA synthesis period; G2, late DNA synthesis; M, mitotic phase.

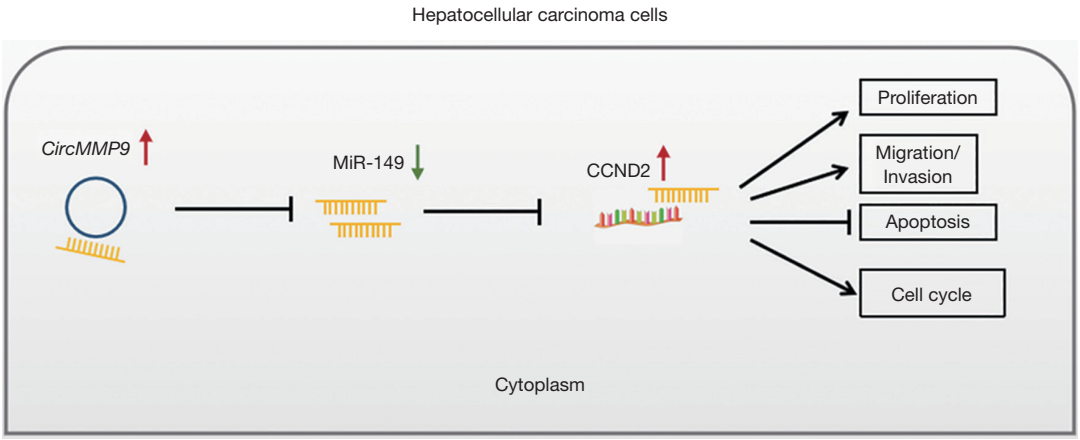

Figure 7 The schematic diagram of this study. *CCND2*, cyclin D2; *circMMP9*, *circular RNA MMP9*.

149 reversed *circMMP9* knockdown-mediated suppression of HCC progression, supporting the notion that *miR-149* is a tumor suppressor.

The miRNAs works as guides via base-pairing with downstream target mRNAs to negatively regulate their expression (45). Various downstream targets of *miR-149* have been identified, such as *PPM1F*, *PARP-2*, *FOXM1*, and *Rap1* (46). In this study, *CCND2* was identified as novel downstream target of *miR-149*. The *miR-149* binds to the 3' UTR of *CCND2* to reduce its expression in HCC. Further, *CCND2* has been proposed to serve as a key regulator in the modulation of cell cycle and proliferation in various cancers (47-49). Consistently, we observed that overexpression of *CCND2* facilitated HCC cell cycle and proliferation. However, further studies were required to explore *miR-149*-mediated regulation of *CCND2* in detail and downstream signaling of *CCND2* in the progression of HCC.

To summarize, we found that *circMMP9* accelerates the progression of HCC by targeting the *miR-149/CCND2* axis for the first time. Our investigation not only implies a novel regulatory mechanism of HCC progression, but also shows the potency of *circMMP9/miR-149/CCND2* axis to be developed as diagnostic and prognostic markers and therapeutic targets for HCC. However, additional research is required to fully understand the nature of the regulation and more samples from patients with HCC and animal models of HCC should be adopted in future studies to evaluate the roles of the *circMMP9/miR-149/CCND2* axis in HCC for clinical application. In addition, we only identified the *circMMP9/miR-149/CCND2* axis in this study. As a circRNA generally has several target miRNAs and a miRNA also targets various genes, studies are ongoing to explore other potential downstream miRNAs and genes of *circMMP9* in HCC.

Acknowledgments

Funding: None.

Footnote

Reporting Checklist: The authors have completed the ARRIVE reporting checklist. Available at https://jgo.amegroups.com/article/view/10.21037/jgo-22-677/rc

Data Sharing Statement: Available at https://jgo.amegroups.com/article/view/10.21037/jgo-22-677/dss

Conflicts of Interest: All authors have completed the ICMJE uniform disclosure form (available at https://jgo.amegroups.com/article/view/10.21037/jgo-22-677/coif). The authors have no conflicts of interest to declare.

Ethical Statement: The authors are accountable for all aspects of the work in ensuring that questions related to the accuracy or integrity of any part of the work are appropriately investigated and resolved. The study was conducted in accordance with the Declaration of Helsinki (as revised in 2013). The study was approved by the Institutional Ethics Review Board of Mengchao Hepatobiliary Hospital of Fujian Medical University (No. 2020-035-01) and informed consent was taken from all the patients. All animal procedures were approved by the Animal Care and Use Committee of Fujian Medical

University (No. 2019009), in compliance with the institutional guidelines for the care and use of animals.

References

1. Llovet JM, Kelley RK, Villanueva A, et al. Hepatocellular carcinoma. Nat Rev Dis Primers 2021;7:6.
2. Villanueva A. Hepatocellular Carcinoma. N Engl J Med 2019;380:1450-62.
3. Lee WC, Jeng LB, Chen MF. Estimation of prognosis after hepatectomy for hepatocellular carcinoma. Br J Surg 2002;89:311-6.
4. Ren Z, Ma X, Duan Z, et al. Diagnosis, Therapy, and Prognosis for Hepatocellular Carcinoma. Anal Cell Pathol (Amst) 2020;2020:8157406.
5. Greene J, Baird AM, Brady L, et al. Circular RNAs: Biogenesis, Function and Role in Human Diseases. Front Mol Biosci 2017;4:38.
6. Memczak S, Jens M, Elefsinioti A, et al. Circular RNAs are a large class of animal RNAs with regulatory potency. Nature 2013;495:333-8.
7. Kristensen LS, Hansen TB, Venø MT, et al. Circular RNAs in cancer: opportunities and challenges in the field. Oncogene 2018;37:555-65.
8. Pan G, Hu T, Chen X, et al. Upregulation Of circMMP9 Promotes Osteosarcoma Progression Via Targeting miR-1265/CHI3L1 Axis. Cancer Manag Res 2019;11:9225-31.
9. Wang R, Zhang S, Chen X, et al. EIF4A3-induced circular RNA MMP9 (circMMP9) acts as a sponge of miR-124 and promotes glioblastoma multiforme cell tumorigenesis. Mol Cancer 2018;17:166.
10. Qiu L, Xu H, Ji M, et al. Circular RNAs in hepatocellular carcinoma: Biomarkers, functions and mechanisms. Life Sci 2019;231:116660.
11. Lv S, Li Y, Ning H, et al. CircRNA GFRA1 promotes hepatocellular carcinoma progression by modulating the miR-498/NAP1L3 axis. Sci Rep 2021;11:386.
12. He S, Yang J, Jiang S, et al. Circular RNA circ_0000517 regulates hepatocellular carcinoma development via miR-326/IGF1R axis. Cancer Cell Int 2020;20:404.
13. Bushati N, Cohen SM. microRNA functions. Annu Rev Cell Dev Biol 2007;23:175-205.
14. Kulcheski FR, Christoff AP, Margis R. Circular RNAs are miRNA sponges and can be used as a new class of biomarker. J Biotechnol 2016;238:42-51.
15. Lu Q, Liu T, Feng H, et al. Circular RNA circSLC8A1 acts as a sponge of miR-130b/miR-494 in suppressing bladder cancer progression via regulating PTEN. Mol Cancer 2019;18:111.
16. Lee YS, Dutta A. MicroRNAs in cancer. Annu Rev Pathol 2009;4:199-227.
17. Hayes J, Peruzzi PP, Lawler S. MicroRNAs in cancer: biomarkers, functions and therapy. Trends Mol Med 2014;20:460-9.
18. He Y, Yu D, Zhu L, et al. miR-149 in Human Cancer: A Systemic Review. J Cancer 2018;9:375-88.
19. Sánchez-González I, Bobien A, Molnar C, et al. miR-149 Suppresses Breast Cancer Metastasis by Blocking Paracrine Interactions with Macrophages. Cancer Res 2020;80:1330-41.
20. Xu K, Liu X, Mao X, et al. MicroRNA-149 suppresses colorectal cancer cell migration and invasion by directly targeting forkhead box transcription factor FOXM1. Cell Physiol Biochem 2015;35:499-515.
21. Luo G, Chao YL, Tang B, et al. miR-149 represses metastasis of hepatocellular carcinoma by targeting actin-regulatory proteins PPM1F. Oncotarget 2015;6:37808-23.
22. Ando K, Ajchenbaum-Cymbalista F, Griffin JD. Regulation of G1/S transition by cyclins D2 and D3 in hematopoietic cells. Proc Natl Acad Sci U S A 1993;90:9571-5.
23. Zhou J, Ju WQ, Yuan XP, et al. miR-26a regulates mouse hepatocyte proliferation via directly targeting the 3' untranslated region of CCND2 and CCNE2. Hepatobiliary Pancreat Dis Int 2016;15:65-72.
24. Tsutsui M, Iizuka N, Moribe T, et al. Methylated cyclin D2 gene circulating in the blood as a prognosis predictor of hepatocellular carcinoma. Clin Chim Acta 2010;411:516-20.
25. Wang M, Gu B, Yao G, et al. Circular RNA Expression Profiles and the Pro-tumorigenic Function of CircRNA_10156 in Hepatitis B Virus-Related Liver Cancer. Int J Med Sci 2020;17:1351-65.
26. Schmidt KM, Geissler EK, Lang SA. Subcutaneous Murine Xenograft Models: A Critical Tool for Studying Human Tumor Growth and Angiogenesis In Vivo. Methods Mol Biol 2016;1464:129-37.

27. Barrett SP, Salzman J. Circular RNAs: analysis, expression and potential functions. Development 2016;143:1838-47.
28. Dudekula DB, Panda AC, Grammatikakis I, et al. CircInteractome: A web tool for exploring circular RNAs and their interacting proteins and microRNAs. RNA Biol 2016;13:34-42.
29. Asafo-Agyei KO, Samant H. Hepatocellular Carcinoma. In: StatPearls. Treasure Island: StatPearls Publishing, 2021.
30. Brown ZJ, Yu SJ, Heinrich B, et al. Indoleamine 2,3-dioxygenase provides adaptive resistance to immune checkpoint inhibitors in hepatocellular carcinoma. Cancer Immunol Immunother 2018;67:1305-15.
31. de la Peña M, Ceprián R, Cervera A. A Singular and Widespread Group of Mobile Genetic Elements: RNA Circles with Autocatalytic Ribozymes. Cells 2020;9:2555.
32. Chen X, Ye Q, Chen Z, et al. Long non-coding RNA muskelin 1 antisense RNA as a potential therapeutic target in hepatocellular carcinoma treatment. Bioengineered 2022;13:12237-47.
33. Lin X, Xiang X, Feng B, et al. Targeting Long Non-Coding RNAs in Hepatocellular Carcinoma: Progress and Prospects. Front Oncol 2021;11:670838.
34. Chen Y, Yuan B, Wu Z, et al. Microarray profiling of circular RNAs and the potential regulatory role of hsa_circ_0071410 in the activated human hepatic stellate cell induced by irradiation. Gene 2017;629:35-42.
35. Cui S, Qian Z, Chen Y, et al. Screening of up- and downregulation of circRNAs in HBV-related hepatocellular carcinoma by microarray. Oncol Lett 2018;15:423-32.
36. Fu L, Yao T, Chen Q, et al. Screening differential circular RNA expression profiles reveals hsa_circ_0004018 is associated with hepatocellular carcinoma. Oncotarget 2017;8:58405-16.
37. Ng WL, Mohd Mohidin TB, Shukla K. Functional role of circular RNAs in cancer development and progression. RNA Biol 2018;15:995-1005.
38. Liu H, Lan T, Li H, et al. Circular RNA circDLC1 inhibits MMP1-mediated liver cancer progression via interaction with HuR. Theranostics 2021;11:1396-411.
39. Yin Y, Long J, He Q, et al. Emerging roles of circRNA in formation and progression of cancer. J Cancer 2019;10:5015-21.
40. Huang G, Liang M, Liu H, et al. CircRNA hsa_circRNA_104348 promotes hepatocellular carcinoma progression through modulating miR-187-3p/RTKN2 axis and activating Wnt/β-catenin pathway. Cell Death Dis 2020;11:1065.
41. Han D, Li J, Wang H, et al. Circular RNA circMTO1 acts as the sponge of microRNA-9 to suppress hepatocellular carcinoma progression. Hepatology 2017;66:1151-64.
42. Salmena L, Poliseno L, Tay Y, et al. A ceRNA hypothesis: the Rosetta Stone of a hidden RNA language? Cell 2011;146:353-8.
43. Verduci L, Strano S, Yarden Y, et al. The circRNA-microRNA code: emerging implications for cancer diagnosis and treatment. Mol Oncol 2019;13:669-80.
44. Xia B, Hong T, He X, et al. A circular RNA derived from MMP9 facilitates oral squamous cell carcinoma metastasis through regulation of MMP9 mRNA stability. Cell Transplant 2019;28:1614-23.
45. Macfarlane LA, Murphy PR. MicroRNA: Biogenesis, Function and Role in Cancer. Curr Genomics 2010;11:537-61.
46. Xu Y, Chen X, Lin L, et al. MicroRNA-149 is associated with clinical outcome in human neuroblastoma and modulates cancer cell proliferation through Rap1 independent of MYCN amplification. Biochimie 2017;139:1-8.
47. Park SY, Lee CJ, Choi JH, et al. The JAK2/STAT3/CCND2 Axis promotes colorectal Cancer stem cell persistence and radioresistance. J Exp Clin Cancer Res 2019;38:399.
48. Ding ZY, Li R, Zhang QJ, et al. Prognostic role of cyclin D2/D3 in multiple human malignant neoplasms: A systematic review and meta-analysis. Cancer Med 2019;8:2717-29.
49. Chang L, Guo R, Yuan Z, et al. LncRNA HOTAIR Regulates CCND1 and CCND2 Expression by Sponging miR-206 in Ovarian Cancer. Cell Physiol Biochem 2018;49:1289-303.

(English Language Editor: J. Jones)

Cite this article as: Li X, Fang J, Wei G, Chen Y, Li D. *CircMMP9* accelerates the progression of hepatocellular carcinoma through the *miR-149/CCND2* axis. J Gastrointest Oncol 2022;13(4):1875-1888. doi: 10.21037/jgo-22-677

